Lecture notes: Reaction-Diffusion Equations and Pattern Formation

A. C. Quillen

August 9, 2025

Contents

1 Reaction-Diffusion equations

Alan Turing found mathematical models that would produce spatial patterns from arbitrary initial states. These models were based on coupled chemical reactions but have since been applied in numerous fields.

1.0.1 The diffusion or heat equation

Let $u(\mathbf{x}, t)$ be a concentration of something, e.g., numbers of molecules per unit volume. The concentration is a function of position $\mathbf{x}$ and time t. The position $\mathbf{x} \in \mathbb{R}^d$ for some dimension d.

The gradient of the concentration of u is $\boldsymbol{\nabla} u$. The rate of flow $\mathbf{F}$ or flux of u should depend on the gradient $\mathbf{F} = -D\boldsymbol{\nabla} u$ with positive coefficient D. The rate of change of u depends on the divergence of the flux or

$$\frac{\partial u}{\partial t} = -\boldsymbol{\nabla} \cdot \mathbf{F}.$$

We expect there to be change in the local quantity of u only if there is variation in the gradient of the flux. If the coefficient D is independent of position then we find

$$\frac{\partial u}{\partial t} = D\nabla^2 u$$

which is known as the diffusion equation or if we replace u with temperature T, it is called the heat equation.

1.0.2 Reaction Diffusion equations

Consider u and v to be concentrations of two chemicals. This means $u \geq 0$ and $v \geq 0$. The chemicals can diffuse through space and they can react with one another and with other

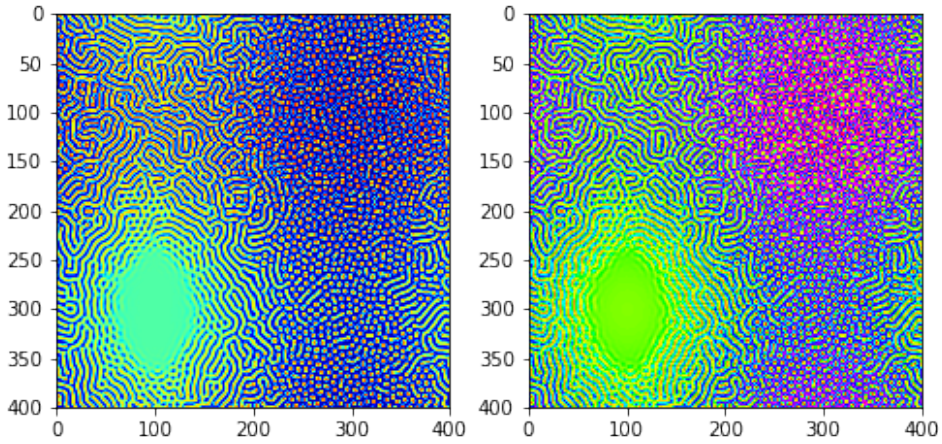

Figure 1: Patterns formed with the Brusselator model. u is on the left and v on the right. The grid has a sinusoidal variation in α (horizontally on the grid) and β (vertically on the grid). The mean values are $\alpha_m = 5$ and $\beta_m = 9$ with amplitudes of variation 1 and 1. Diffusion coefficients are $D_u = 2, D_v = 22$, the grid is $n = 400$ grid points and square and $\Delta x = 1, \Delta t = 0.0025$. The axes are x, y. Boundary conditions are periodic. The patterns grow and then become fixed.

reagents.

$$\frac{\partial u}{\partial t} = D_u \nabla^2 u + f_u(u, v) \tag{1}$$

$$\frac{\partial v}{\partial t} = D_v \nabla^2 v + f_v(u, v). \tag{2}$$

Here D_u, D_v are the diffusion coefficients for u and v respectively. The functions $f_u(u, v)$ and $f_v(u, v)$ are the local reaction rates. In two dimensions $u(x, y, t)$ and $v(x, y, t)$ and the Laplacian operator

$$\Delta = \nabla^2 = \frac{\partial^2}{\partial x^2} + \frac{\partial^2}{\partial y^2}. \tag{3}$$

1.1 The Brusselator model

The Brusselator model (developed by a group in Brussels) has reactions

$$\begin{aligned} \alpha &\to u \\ \beta + u &\to v \\ 2u + v &\to 3u \\ u &\to E \end{aligned}$$

where the concentrations of the reagents $\alpha, \beta, E \geq 0$ are kept constant. The reactions together give

$$f_u(u,v) = \alpha - (\beta+1)u + u^2 v$$
$$f_v(u,v) = \beta u - u^2 v. \tag{4}$$

Here α is a feeding rate for u. The parameter β is a kill rate for u that converts u to v. The uv^2 term is a reaction term, producing u at the expense of v.

Allowing u, v to also diffuse

$$\frac{\partial u}{\partial t} = D_u \nabla^2 u + \alpha - (\beta+1)u + u^2 v \tag{5}$$
$$\frac{\partial v}{\partial t} = D_v \nabla^2 v + \beta u - u^2 v. \tag{6}$$

This set of coupled equations displays a variety of phenomena, including growth of patterns (see Figure 1) and long lived oscillating behavior (see Figure 3).

1.1.1 The steady state of the Brusselator model

We consider the reaction alone. What is the steady state solution? The steady state solution satisfies

$$f_u(u,v) = \alpha - (\beta+1)u + u^2 v = 0$$
$$f_v(u,v) = \beta u - u^2 v = 0$$

The second equation gives $\beta = uv$ and this in the first equation gives $\alpha = u$ and consequently $v = \beta/\alpha$. The steady state solution is

$$u_0 = \alpha$$
$$v_0 = \frac{\beta}{\alpha}. \tag{7}$$

We can consider trajectories on the u, v plane. The steady state solution is a fixed point.

1.2 Wavelengths of the patterns that grow

To try to understand which types of patterns grow we look at the stability of perturbations near the steady state solution. Using linearized equations we estimate the growth rate as a function of wavevector or wavelength.

1.2.1 Linear perturbations near the steady state solution for the Brusselator model

We assume a solution that is near the steady state solution.

$$\begin{aligned} u(x,y,t) &= u_0 + u_1(x,y,t) \\ v(x,y,t) &= v_0 + v_1(x,y,t), \end{aligned} \tag{8}$$

where the steady state solution satisfies

$$\begin{aligned} f_u(u_0, v_0) &= 0 \\ f_v(u_0, v_0) &= 0. \end{aligned}$$

We expand the equations of motion to first order in u_1, v_1, assuming that they are small.

We write down the equation of motion again (equation 6)

$$\frac{\partial u}{\partial t} = D_u \nabla^2 u + \alpha - (\beta + 1)u + u^2 v \tag{9}$$

$$\frac{\partial v}{\partial t} = D_v \nabla^2 v + \beta u - u^2 v. \tag{10}$$

Here is how to compute the non-linear terms

$$\begin{aligned} u^2 v &= (u_0 + u_1)^2 (v_0 + v_1) \\ &= (u_0^2 + 2u_0 u_1 + u_1^2)(v_0 + v_1) \\ &= u_0^2 v_0 + 2u_0 u_1 v_0 + u_1^2 v_0 + u_0^2 v_1 + 2u_0 u_1 v_1 + u_1^2 v_1 \\ &= u_0^2 v_0 + 2u_0 v_0 v_1 + u_0^2 v_1 + ... \end{aligned}$$

The first order terms are $2u_0 v_0 v_1 + u_0^2 v_1$.

We plug equations 8 into the equations of motion and only keep zeroth and first order terms

$$\begin{aligned} u_{0,t} + u_{1,t} &= D_u(u_{0,xx} + u_{1,xx} + u_{0,yy} + u_{1,yy}) + \alpha - (\beta + 1)(u_0 + u_1) + u_0^2 v_0 + 2u_0 v_0 v_1 + u_0^2 v_1 \\ v_{0,t} + v_{1,t} &= D_v(v_{0,xx} + v_{1,xx} + v_{0,yy} + v_{1,yy}) + \beta(u_0 + u_1) - u_0^2 v_0 - 2u_0 v_0 v_1 + u_0^2 v_1. \end{aligned}$$

The steady state solution in independent of position so it has $u_{0,xx} = 0$, $u_{0,yy} = 0$, $u_{0,t} = 0$ and $v_{0,xx} = 0$, $v_{0,yy} = 0$, $v_{0,xx} = 0$. Deleting those terms we get

$$\begin{aligned} u_{1,t} &= D_u(u_{1,xx} + u_{1,yy}) - (\beta + 1)u_1 + 2u_0 v_0 v_1 + u_0^2 v_1 + \alpha - (\beta + 1)u_0 + u_0^2 v_0 \\ v_{1,t} &= D_v(v_{1,xx} + v_{1,yy}) + \beta u_1 - u_0^2 v_0 - 2u_0 v_0 v_1 + u_0^2 v_1 + \beta u_0 - u_0^2 v_0. \end{aligned}$$

The terms that are zeroth order now drop out precisely because they involve the steady state solution. We delete the zero-th order terms. To first order in u_1, v_1 and in two dimensions the equations of motion for the Brusselator model are

$$u_{1,t} = D_u(u_{1,xx} + u_{1,yy}) - (\beta + 1)u_1 + u_0^2 v_1 + 2u_0 v_0 u_1$$
$$v_{1,t} = D_v(v_{1,xx} + v_{1,yy}) + \beta u_1 - u_0^2 v_1 - 2u_0 v_0 u_1.$$

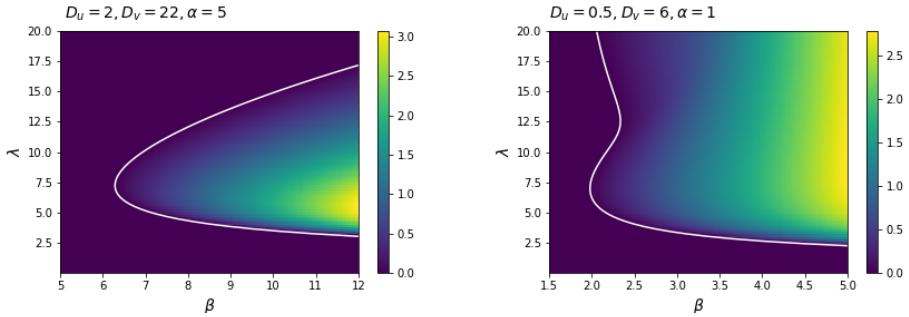

Figure 2: The real part $\gamma_+(k)$ giving the growth rate of perturbations for the Brusselator model. The left axis shows the wavelength $\lambda = 2\pi/k$. The diffusion coefficients and α are fixed and equation 14 used to compute the growth rate as a function of wave-vector k and parameter β. The parameter α and diffusion coefficients are printed on the top of the figures. Negative portions of the images are not shown. The white lines show zero growth rate. If the diffusion coefficients are reduced, smaller wavelengths can become unstable.

Using the steady state solution this becomes

$$u_{1,t} = D_u(u_{1,xx} + u_{1,yy}) + (\beta - 1)u_1 + \alpha^2 v_1$$
$$v_{1,t} = D_v(v_{1,xx} + v_{1,yy}) - \beta u_1 - \alpha^2 v_1.$$

We adopt a trial solution in the form

$$u_1 = \tilde{u}_1 e^{\gamma t + ik_x x + ik_y y}$$
$$v_1 = \tilde{v}_1 e^{\gamma t + ik_x x + ik_y y}$$

giving

$$\left[\gamma + D_u(k_x^2 + k_y^2) - (\beta - 1)\right] \tilde{u}_1 = \alpha^2 \tilde{v}_1$$
$$\left[\gamma + D_v(k_x^2 + k_y^2) + \alpha^2\right] \tilde{v}_1 = -\beta \tilde{u}_1.$$

We combine these together to find

$$\left[\gamma + D_u(k_x^2 + k_y^2) - (\beta - 1)\right] \left[\gamma + D_v(k_x^2 + k_y^2) + \alpha^2\right] + \alpha^2 \beta = 0$$

This can be called the 'characteristic equation'.

The characteristic equation is a quadratic equation for γ that is a function of $k^2 = k_x^2 + k_y^2$ and parameters α, β. This characteristic equation can be written in the form

$$\gamma^2 + B(k)\gamma + C(k) = 0 \tag{11}$$

with coefficients

$$B(k) = (D_u + D_v)k^2 + \alpha^2 - \beta + 1 \tag{12}$$

$$C(k) = D_u D_v k^4 + D_u k^2 \alpha^2 + D_v k^2 (1 - \beta) + \alpha^2. \tag{13}$$

The quadratic formula

$$\gamma(k) = -\frac{B(k)}{2} \pm \frac{1}{2}\sqrt{B^2(k) - 4C(k)}. \tag{14}$$

If there are values of wave vector k giving solutions for γ that have a positive real part, these would correspond to perturbations that can grow exponentially quickly.

What wavevectors give a zero growth rate? These can be considered transition regions and they would satisfy $C(k) = 0$.

Because $B(k), C(k)$ are real functions, the larger of the two possible values for Reγ

$$\mathrm{Re}\gamma_+(k) = \begin{cases} -\frac{B(k)}{2} + \frac{1}{2}\sqrt{B^2(k) - 4C(k)} & \text{if} \quad B^2(k) - 4C(k) \geq 0 \\ -\frac{B(k)}{2} & \quad\quad\; B^2(k) - 4C(k) < 0 \end{cases} \tag{15}$$

The Brusselator model is specified by four parameters D_u, D_v, α, β, but growth rate γ_+ also depends on k. If you fix three of the parameters, say D_u, D_v, α, you can show the value of Reγ_+ on a two-d plot with the other two degrees of freedom β, k as axes. Where this is positive, you expect growth of structure with wavelength $\lambda = 2\pi/k$ and with growth rate given by Reγ_+. See Figure 2 for some plots of Reγ_+.

1.2.2 Linear analysis with a Jacobian

Using reaction functions to first order about the steady state solution

$$f_u(u_0 + u_1, v_0 + v_1) = f_u(u_0, v_0) + \left.\frac{\partial f_u}{\partial u}\right|_{u_0,v_0} u_1 + \left.\frac{\partial f_u}{\partial v}\right|_{u_0,v_0} v_1$$

$$f_v(u_0 + u_1, v_0 + v_1) = f_v(u_0, v_0) + \left.\frac{\partial f_v}{\partial u}\right|_{u_0,v_0} u_1 + \left.\frac{\partial f_v}{\partial v}\right|_{u_0,v_0} v_1.$$

Let $\mathbf{u} = (u, v)$ and $\mathbf{f}(\mathbf{u}) = (f_u(\mathbf{u}), f_v(\mathbf{u}))$. The steady state solution $\mathbf{u}_0$ satisfies $\mathbf{f}(\mathbf{u}_0) = 0$. Expanding about the steady state solution

$$\mathbf{f}_u(\mathbf{u}_0 + \mathbf{u}_1) = \mathbf{f}_u(\mathbf{u}_0) + \left.\mathbf{Df}\right|_{\mathbf{u}_0} \mathbf{u}_1 + ...$$

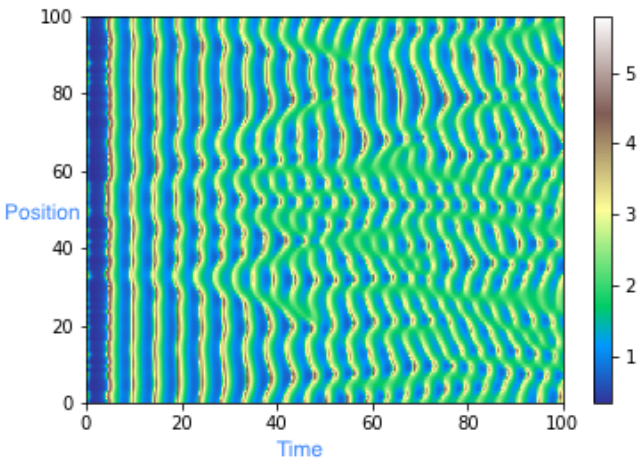

Figure 3: The Brusselator model in 1-dimension integrated with $D_u = 0.3, D_v = D_u/8$, $\alpha = 2$, $\beta = 5.4$, $\Delta x = 1$, $\Delta t = 0.005$. The horizontal axis is time, and the vertical axis is x. The boundary condition is periodic. This shows both development of spatial patterns and time dependent structures.

where $\mathbf{Df}$ is the Jacobian matrix. For the Brusselator model, the Jacobian matrix

$$\begin{aligned}\mathbf{Df} &= \begin{pmatrix} \frac{\partial f_u}{\partial u} & \frac{\partial f_u}{\partial v} \\ \frac{\partial f_v}{\partial u} & \frac{\partial f_v}{\partial v} \end{pmatrix} \\ &= \begin{pmatrix} -(\beta+1)+2uv & u^2 \\ \beta - 2uv & -u^2 \end{pmatrix}.\end{aligned}$$

Evaluated at the steady state solution or fixed point (equation 7) the Jacobian matrix

$$\mathbf{Df}\Big|_{\mathbf{u}_0} = \begin{pmatrix} \beta - 1 & \alpha^2 \\ -\beta & -\alpha^2 \end{pmatrix}. \tag{16}$$

The equation of motion in vector form

$$\frac{\partial \mathbf{u}}{\partial t} = \begin{pmatrix} D_u & 0 \\ 0 & D_v \end{pmatrix} \Delta \mathbf{u} + \mathbf{f}(\mathbf{u}) \tag{17}$$

where the Laplacian operator $\Delta = \frac{\partial^2}{\partial x^2} + \frac{\partial^2}{\partial y^2}$. To first order in $\mathbf{u}_1$ and expanded about the steady state solution, the equation of motion is

$$\frac{\partial \mathbf{u}_1}{\partial t} = \begin{pmatrix} D_u & 0 \\ 0 & D_v \end{pmatrix} \Delta \mathbf{u}_1 + \mathbf{Df}\Big|_{\mathbf{u}_0} \mathbf{u}_1.$$

With trial solution $\mathbf{u}_1 = \tilde{\mathbf{u}}_1 e^{\gamma t + i\mathbf{k}\cdot\mathbf{x}}$ with $\mathbf{k} = (k_x, k_y)$ and $\mathbf{x} = (x, y)$ the first order equation gives

$$\gamma\tilde{\mathbf{u}}_1 = \left[-\begin{pmatrix} D_u & 0 \\ 0 & D_v \end{pmatrix} k^2 + \mathbf{Df}\Big|_{\mathbf{u}_0} \right] \tilde{\mathbf{u}}_1.$$

This can be rewritten with an identity matrix $\mathbf{I}$

$$\left[-\begin{pmatrix} D_u & 0 \\ 0 & D_v \end{pmatrix} k^2 + \mathbf{Df}\Big|_{\mathbf{u}_0} - \gamma\mathbf{I} \right] \tilde{\mathbf{u}}_1 = 0 \tag{18}$$

The thing inside the brackets is a matrix. We find the characteristic equation by taking the determinant of the matrix and setting it to zero;

$$\det\left[\begin{pmatrix} \gamma + D_u k^2 & 0 \\ 0 & \gamma + D_v k^2 \end{pmatrix} - \mathbf{Df}\Big|_{\mathbf{u}_0} \right] = 0.$$

For the Brusselator model and using equation 16 for the Jacobian matrix

$$\det\left[\begin{pmatrix} \gamma + D_u k^2 & 0 \\ 0 & \gamma + D_v k^2 \end{pmatrix} - \begin{pmatrix} \beta - 1 & \alpha^2 \\ -\beta & -\alpha^2 \end{pmatrix} \right] = 0. \tag{19}$$

This gives the following equation for the growth rate $\gamma(k)$

$$\left(\gamma + D_u k^2 - \beta + 1\right)\left(\gamma + D_v k^2 + \alpha^2\right) + \alpha^2\beta = 0. \tag{20}$$

We find the same characteristic equation as we derived in the last section but using different notation. As discussed in the last section, solutions to the characteristic equation tell you whether small perturbations can grown. If the real part of $\gamma(k)$ is positive then perturbations with wavelength $2\pi/k$ are likely to grow. The linear analysis does not tell you what types of patterns (like dots or ridges or spirals) are likely to form.

1.3 Temporal behavior of the Brusselator model

We consider the Brusselator model near its steady state solution. The steady state solution may not be stable. Without diffusion, the Brusselator model

$$\begin{aligned} \frac{\partial u}{\partial t} &= f_u(u, v) \\ \frac{\partial v}{\partial t} &= f_v(u, v) \end{aligned}$$

with reaction functions in equation 4 which we repeat here

$$\begin{aligned} f_u(u, v) &= \alpha - (\beta + 1)u + u^2 v \\ f_v(u, v) &= \beta u - u^2 v. \end{aligned}$$

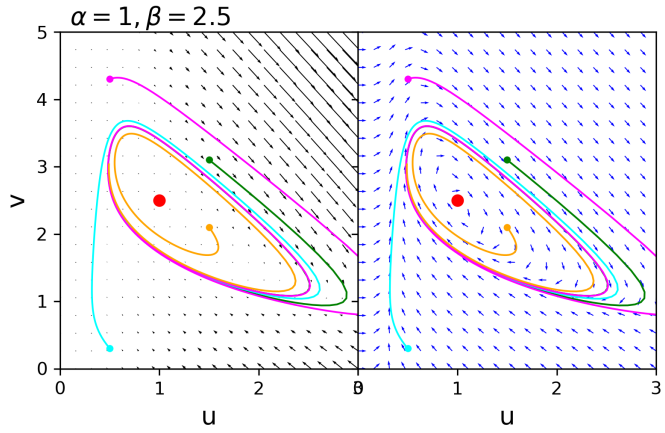

Figure 4: Trajectories in u, v space for the Brusselator model taking into account only evolution in u, v (without diffusion). The parameters $\alpha = 1, \beta = 2.5$. The fixed point is shown with a red dot and is unstable. Orbits are shown with colored lines. Arrows on the left show vectors $(\frac{du}{dt}, \frac{dv}{dt})$. Arrows on the right show the same vectors but normalized so that they all have the same length. Orbits are attracted to a limit cycle giving periodic behavior.

On a plot of u vs v, the point u_0, v_0 is a fixed point.

We look at trajectories near the steady state solution u_0, v_0. Let $u = u_0 + u_1$ and $v = v_0 + v_1$. The equations of motion expanded about the fixed point

$$\frac{\partial u_1}{\partial t} = f_u(u_0, v_0) + \frac{\partial f_u}{\partial u}\Big|_{u_0,v_0} u_1 + \frac{\partial f_u}{\partial v}\Big|_{u_0,v_0} v_1$$
$$\frac{\partial v_1}{\partial t} = f_v(u_0, v_0) + \frac{\partial f_v}{\partial u}\Big|_{u_0,v_0} u_1 + \frac{\partial f_v}{\partial v}\Big|_{u_0,v_0} v_1$$

The terms $f_u(u_v, v_0) = 0$ and $f_v(u_v, v_0) = 0$ because u_0, v_0 give the steady state solution. The above equation can be written in vector form with $\mathbf{w} = \begin{pmatrix} u_1 \\ v_1 \end{pmatrix}$ as

$$\frac{\partial \mathbf{w}}{\partial t} = \mathbf{J}\mathbf{w} \tag{21}$$

with $\mathbf{J}$ the Jacobian matrix evaluated at $\mathbf{w}_0 = (u_0, v_0)$.

Let us look at the Jacobian matrix computed at the fixed point (equation 16) for the Brusselator model, repeated here

$$\mathbf{J} = \mathbf{Df}\Big|_{\mathbf{w}_0} = \begin{pmatrix} \beta - 1 & \alpha^2 \\ -\beta & -\alpha^2 \end{pmatrix}. \tag{22}$$

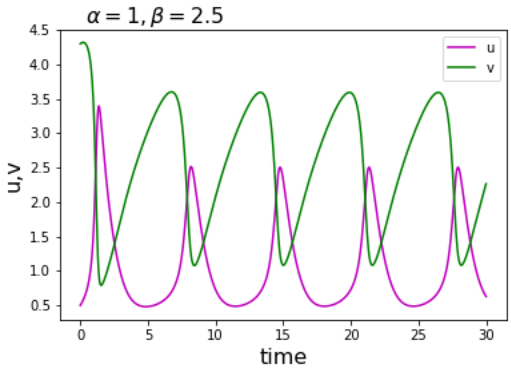

Figure 5: Time evolution of u, v in the Brusselator model (without any diffusion and at a single point) for $\alpha = 1, \beta = 2.5$, showing a limit cycle.

Consider an eigenvector $\mathbf{w}_\lambda$ of the Jacobian matrix $\mathbf{J}$ with eigenvalue λ. Because it is an eigenvector

$$\mathbf{J}\mathbf{w}_\lambda = \lambda \mathbf{w}_\lambda$$

and equation 21 has solution

$$\mathbf{w}(t) = \mathbf{w}_\lambda e^{\lambda t}.$$

If the eigenvalue has a real positive part then the solution near the fixed point moves away from the fixed point. If the eigenvalue has a real negative part then the solution moves toward the fixed point.

To help us compute the eigenvalues of the Jacobian matrix for the Brusselator model, we compute its trace and determinant

$$\begin{aligned} \mathrm{tr}\mathbf{J} &= \beta - 1 - \alpha^2 \\ \det\mathbf{J} &= \alpha^2. \end{aligned} \tag{23}$$

We can compute the eigenvalues of the Jacobian matrix. The eigenvalues of a 2x2 matrix in terms of its trace and determinant

$$\begin{aligned} \lambda_\pm &= \frac{1}{2}\left(\mathrm{tr}A + \sqrt{\mathrm{tr}A - 4\ \det A}\right) \\ &= \frac{1}{2}\left(\beta - 1 - \alpha^2 \pm \sqrt{(\beta - 1 - \alpha^2)^2 - 4\alpha^2}\right). \end{aligned} \tag{24}$$

The trace is the sum of the two eigenvalues and the determinant is the product of the two eigenvalues. If both trace and determinant are positive the fixed point is a repeller and is not stable.

Equations 23 and 24 show that the fixed point is unstable with positive real parts for both eigenvalues if tr$\mathbf{J} > 0$. This condition is

$$\beta - 1 - \alpha^2 > 0 \tag{25}$$

or equivalently

$$\beta > 1 + \alpha^2. \tag{26}$$

If the two eigenvalues are complex then the unstable fixed point has circulation and can give birth to a limit cycle (see Figures 4 and 5). The eigenvalues have a complex part if the quantity inside the square root (in equation 24) is negative or

$$2\alpha > \beta - 1 - \alpha^2,$$

where I assumed the sign for $(\beta - 1 - \alpha^2)$ giving instability from equation 25. Equivalently for the eigenvalues to have complex parts we require

$$\beta < (1 + \alpha)^2. \tag{27}$$

Combining equations 26 and 27, the fixed point is both unstable and has complex eigenvalues, (giving birth to a limit cycle and with what is known as a *Hopf bifurcation*) if

$$1 + \alpha^2 > \beta > (1 + \alpha)^2. \tag{28}$$

We will get interesting temporal behavior in the Brusselator model if this condition is satisfied.

We should have discussed the global morphology of the system (see Figure 6). For a limit cycle to appear, the dynamical system must be sufficiently non-linear that distant from the fixed point, trajectories move or contract toward the fixed point. We could make a quiver plot of the vector $\dot{u}, \dot{v}$ on the u, v plane to show that trajectories tend to circulate and move inwards at large values of u, v. Then orbits move away from the fixed point near the fixed point and move toward it at large distances from it. The attracting stable trajectory is a **limit cycle** which looks like a loop on the u, v plane, as shown in Figure 4 and gives periodic behavior for u and v, as shown in Figure 5 and Figure 6.

1.4 Temporal or Turing instability

For the Brusselator model Turing instability (giving growth of spatial patterns) can occur[1] for

$$\beta < (1 + \eta\alpha)^2\eta \equiv \sqrt{\frac{D_u}{D_v}} < \sqrt{1 + \alpha^2} - 1 \tag{29}$$

[1] G. Nicolis, Introduction to Nonlinear Science (Cambridge University Press, Cambridge, 1995). or J. Verdasca, A. D. Wit, G. Dewel, and P. Borckmans, Physics Letters A 168, 194 (1992). or B. Pena and C. Perez-Garcia, Physical Review E 64, 056213 (2001).

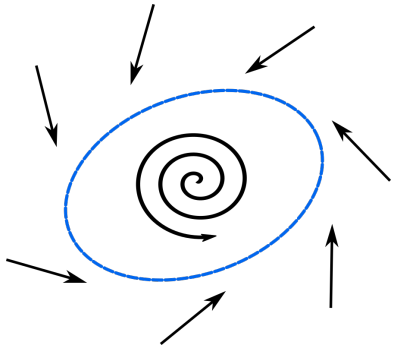

Figure 6: The fixed point at the center is an unstable spiral. At large distances from the fixed points orbits contract toward the fixed point. Orbits must be attracted to the limit cycle which is shown in blue. The axis would be u, v and the arrows show the vector $\left(\frac{\partial u}{\partial t}, \frac{\partial v}{\partial t}\right)$.

For the Brusselator model temporal instability (sometimes called Hoft instability) occurs in a different region of parameter space than Turing instability. Other dynamical systems, including some reaction diffusion pattern formation models can exhibit **chimera** states[2] where both temporal instability and growth of spatial patterns can occur.

1.5 Numerical implementation on a Cartesian grid

We model a reaction diffusion system discretely in both space and time.

In two dimensions we make an evenly spaced grid for the u, v values. The 2-dimensional spatial grid is specified by indices i, j where $i = 0, 1, ..., N-1$ and $j = 0, 1, ..., N-1$ for an $N \times N$ grid. The value of u at the i, j grid point is u_{ij} and the value of v is v_{ij}. The distance between consecutive grid points in either x or y directions is Δx.

We also discretize the system in time. We specify u, v values at evenly spaced times or separated in time by a time-step Δt. The value of u_{ij} at the n-th time-step is u^n_{ij}.

1.5.1 The Laplacian operator

Note, we have used $\Delta x, \Delta t$ to represent grid spacing and time step. However Δ is also often used to represent the Laplacian operator.

[2] Y. Kuramoto and D. Battogtokh, Coexistence of coherence and incoherence in nonlocally coupled phase oscillators. Nonlinear Phenom. Complex Syst. 5, 380 (2002). D. M. Abrams and S. H. Strogatz, Chimera states for coupled oscillators. Phys. Rev. Lett. 93, 174102 (2004). Spiral wave chimeras in reaction-diffusion systems: phenomenon, mechanism and transitions, Li et al. 2020, arXiv:2012.00983

On a 1 dimensional spatial grid we can approximate the second derivative

$$\frac{\partial^2 u_j}{\partial x^2} \approx \frac{u_{j+1} + u_{j-1} - 2u_j}{(\Delta x)^2}. \tag{30}$$

We explain why this is an approximation by expanding $u(x)$ in a Taylor series

$$\begin{aligned} u(x + \Delta x) &= u(x) + u'(x)\Delta x + u''(x)\frac{(\Delta x)^2}{2} + \mathcal{O}(\Delta x^3) + ... \\ u_{j+1} &= u_j + u'_j\Delta x + u''_j\frac{(\Delta x)^2}{2} + \mathcal{O}(\Delta x^3) + ... \\ u_{j-1} &= u_j - u'_j\Delta x + u''_j\frac{(\Delta x)^2}{2} + \mathcal{O}(\Delta x^3) + ... \\ u_{j+1} + u_{j-1} - 2u_j &= u''_j\Delta x^2 + \mathcal{O}(\Delta x^3) + ... \end{aligned}$$

This lets us see not only that equation 30 is an approximation but also how accurate it is.

The two dimensional Laplacian

$$\frac{\partial^2 u_{ij}}{\partial x^2} + \frac{\partial^2 u_{ij}}{\partial y^2} \approx \frac{u_{i,j+1} + u_{i,j-1} + u_{i+1,j} + u_{i-1,j} - 4u_{ij}}{(\Delta x)^2} \tag{31}$$

Notice that the Laplacian is a linear operator that operates on u. Given a vector of u values, one can write the discrete operator as a sparse matrix.

1.5.2 A first order forward Eulerian method

We describe an Eulerian scheme to update the grid at the next time step using the u, v values at the current time step. We approximate the time derivative

$$\frac{\partial u^n_{ij}}{\partial t} \approx \frac{u^{n+1}_{ij} - u^n_{ij}}{\Delta t}$$

This gives

$$u^{n+1}_{ij} = u^n_{ij} + \Delta t \ \frac{\partial u^n_{ij}}{\partial t}.$$

The time derivative on the right is specified by the right hand side for our equations of motion. The full scheme is then

$$\begin{aligned} u^{n+1}_{ij} &= u^n_{ij} + \Delta t \left(D_u \frac{u^n_{i,j+1} + u^n_{i,j-1} + u^n_{i+1,j} + u^n_{i-1,j} - 4u^n_{ij}}{(\Delta x)^2} + f_u(u^n_{ij}, v^n_{ij}) \right) \\ v^{n+1}_{ij} &= v^n_{ij} + \Delta t \left(D_v \frac{u^n_{i,j+1} + u^n_{i,j-1} + u^n_{i+1,j} + u^n_{i-1,j} - 4u^n_{ij}}{(\Delta x)^2} + f_v(u^n_{ij}, v^n_{ij}) \right) \end{aligned}$$

where f_u, f_v are the reaction rate functions. Starting with some initial conditions for u, v 2-dimensional arrays, we can using this equation to compute new arrays for u, v consecutively for each time-step.

1.5.3 Fitting the pattern into the domain and grid or element space

To see patterns the most unstable wavelength should fit within the domain.

Also the distance between grid points or the size of your elements should be smaller than the most unstable wavelength.

The only terms in the reaction diffusion equation that contain spatial dimensions are the diffusive terms. Hence, scaling your domain is equivalent to rescaling the diffusion coefficients.

1.5.4 Initial conditions

Reaction-diffusion equations can be sensitive to initial conditions. For the Brusselator model, I find I tend to get nice patterns with u, v small but randomly chosen. For example, u, v values on the grid chosen from uniform distributions in $[0, 0.05)$.

For the Gray-Scott model, I find that the v field should be seeded with a few positions that have $v = 1$ to get interesting patterns.

1.5.5 Periodic boundary conditions

Boundary conditions can affect the behavior of the model. The easiest type of boundary condition to implement numerically is the periodic boundary condition where we take i and j modulo N (the grid length) when computing the Laplacian.

1.5.6 Numerical Stability

The Eulerian updating scheme will not be be stable unless we keep

$$\Delta t \lesssim \frac{(\Delta x)^2}{\max(D_u, D_v)}. \tag{32}$$

For the diffusion equation, this can be shown using von-Neumann stability analysis.[3] Physically this condition can be understood by considering the time it takes information to travel between grid cells. Diffusion coefficients have units of Length^2/Time and information on the grid travels with scaling similar to that of a random walk. For a random walk, the variance of a number of walkers (a distance squared) is proportional to time. The time required for the bulk of them to travel a particular distance depends on the square of this distance. If the diffusion coefficient is larger or/and the grid spacing is smaller, then the time step must be reduced for the scheme to be numerically stable. If the scheme is unstable you will probably notice because you will get zigzags in u and v and numerical values will then increase rapidly to ∞.

[3] Take a Fourier transform, write the update procedure in terms of a matrix times a vector, then look at eigenvalues of the matrix. If any of the eigenvalues are real and positive, the system is unstable.

The condition is similar to the CFL (Courant-Friedrichs-Lewy) condition for a numerically integrated hydrodynamic system where Δt should be lower than the time it takes for sound waves to travel between grid points.

1.5.7 The Crank-Nicolson method for Diffusion

The Crank Nicolson method is an implicit method which lends itself to using matrix operators during computation. We want to integrate $u(x,t)$ with

$$\partial_t u = F(u, \partial_x u_x, \partial_{xx} u). \tag{33}$$

We take $\mathbf{u}$ to represent a vector of u values at different positions. Equation 33 is approximated by

$$\frac{\mathbf{u}^{n+1} - \mathbf{u}^n}{\Delta t} = \frac{1}{2}\left(\mathbf{F}^{n+1}(u, \partial_x u, \partial_{xx} u) + \mathbf{F}^n(u, \partial_x u, \partial_{xx} u)\right). \tag{34}$$

If the function $\mathbf{F}$ is a linear function of $\mathbf{u}$, when put on a grid (or mesh), this equation becomes a matrix equation. Suppose we can write $\mathbf{F}(u, \partial_x u, \partial_{xx} u) = \mathbf{A}\mathbf{u}$ for some linear operator $\mathbf{A}$. Then equation 36 becomes

$$\frac{\mathbf{u}^{n+1} - \mathbf{u}^n}{\Delta t} = \frac{1}{2}\left(\mathbf{A}\mathbf{u}^{n+1} + \mathbf{A}\mathbf{u}^n\right). \tag{35}$$

With some rearrangement

$$\begin{aligned}
\mathbf{u}^{n+1} - \frac{\Delta t}{2}\mathbf{A}\mathbf{u}^{n+1} &= u^n + \frac{\Delta t}{2}\mathbf{A}\mathbf{u}^n \\
\left(\mathbf{I} - \frac{\Delta t}{2}\mathbf{A}\right)\mathbf{u}^{n+1} &= \left(\mathbf{I} + \frac{\Delta t}{2}\mathbf{A}\right)\mathbf{u}^n \\
\mathbf{u}^{n+1} &= \left(\mathbf{I} - \frac{\Delta t}{2}\mathbf{A}\right)^{-1}\left(\mathbf{I} + \frac{\Delta t}{2}\mathbf{A}\right)\mathbf{u}^n
\end{aligned} \tag{36}$$

where $\mathbf{I}$ is the identity operator. A vector of $\mathbf{u}^{n+1}$ values can be solved in terms of a vector of $\mathbf{u}^n$ values by inverting a matrix that is usually sparse.

How is this method relevant for integrating reaction diffusion systems? The Laplacian operator is a linear operator (determines $\mathbf{A}$).

1.6 Stability of numerical schemes

Can we tell if a numerical scheme is stable? Examine equation 36. On the right hand side is a linear operator that depends upon the time-step Δt. This equation can be written as

$$\mathbf{u}^{n+1} = \mathbf{B}\mathbf{u}^n \tag{37}$$

where $\mathbf{B}$ is a matrix. The stability of the scheme depends upon the eigenvalues of the linear operator $\mathbf{B}$. If there are positive eigenvalues then the scheme can be unstable. The sign of the eigenvalues can depend on the time step which is why many numerical methods require that a CFL like condition is satisfied.

The Crank-Nicolson method is a second order scheme that is numerically stable. A low CFL number is not required for *stability* of the Crank-Nicolson numerical scheme, however, it is required for numerical *accuracy*.

1.6.1 Operator splitting

A possible method is to split the system into two steps, first taking a Crank-Nicolson step for the diffusive part of the reaction diffusion equation. Then afterwards a first order Eulerian step is taken to take into account the reaction terms.

We discretize u (for example, as before on our 2d Cartesian grid) but we flatten it so that it is a vector, one number for each node of our grid or mesh. We write $\mathbf{u}$ to describe this vector. The diffusion part of the reaction diffusion equation is written in terms of a Laplacian operator $\mathbf{L}$ (equation 31) that is a matrix that operates on the vector $\mathbf{u}$. The Crank Nicolson scheme (equation 36) becomes

$$\mathbf{u}^{n+1} = \mathbf{u}^n + \frac{D_u \Delta t}{2}\mathbf{L}\mathbf{u}^{n+1} + \frac{D_u \Delta t}{2}\mathbf{L}\mathbf{u}^n \tag{38}$$

$$\mathbf{v}^{n+1} = \mathbf{v}^n + \frac{D_v \Delta t}{2}\mathbf{L}\mathbf{u}^{n+1} + \frac{D_v \Delta t}{2}\mathbf{L}\mathbf{v}^n \tag{39}$$

Using the identity matrix $\mathbf{I}$ we regroup

$$\left(\mathbf{I} - \frac{D_u \Delta t}{2}\mathbf{L}\right)\mathbf{u}^{n+1} = \left(\mathbf{I} + \frac{D_u \Delta t}{2}\mathbf{L}\right)\mathbf{u}^n \tag{40}$$

and similarly for v. This gives the matrix equation for the $\mathbf{u}^{n+1}$ in terms of $\mathbf{u}^n$

$$\mathbf{u}^{n+1} = \left(\mathbf{I} - \frac{D_u \Delta t}{2}\mathbf{L}\right)^{-1}\left(\mathbf{I} + \frac{D_u \Delta t}{2}\mathbf{L}\right)\mathbf{u}^n \tag{41}$$

$$\mathbf{v}^{n+1} = \left(\mathbf{I} - \frac{D_v \Delta t}{2}\mathbf{L}\right)^{-1}\left(\mathbf{I} + \frac{D_v \Delta t}{2}\mathbf{L}\right)\mathbf{v}^n. \tag{42}$$

Here we have written -1 to denote matrix inversion, but this could also be solved via LU decomposition. Doing both the reaction and diffusive parts of a reaction diffusion equation,

$$\mathbf{u}^{n+1} = \left(\mathbf{I} - \frac{D_u \Delta t}{2}\mathbf{L}\right)^{-1}\left(\mathbf{I} + \frac{D_u \Delta t}{2}\mathbf{L}\right)\mathbf{u}^n + R_u(\mathbf{u}^n, \mathbf{v}^n)\Delta t \tag{43}$$

$$\mathbf{v}^{n+1} = \left(\mathbf{I} - \frac{D_v \Delta t}{2}\mathbf{L}\right)^{-1}\left(\mathbf{I} + \frac{D_v \Delta t}{2}\mathbf{L}\right)\mathbf{v}^n + R_u(\mathbf{u}^n, \mathbf{v}^n)\Delta t. \tag{44}$$

1.7 The Gray-Scott model

The Gray-Scott model has

$$f_u(u,v) = -uv^2 + \alpha(1-u) \tag{45}$$
$$f_v(u,v) = uv^2 - (\alpha+\beta)v \tag{46}$$

and

$$\frac{\partial u}{\partial t} = D_u\nabla^2 u - uv^2 + \alpha(1-u) \tag{47}$$
$$\frac{\partial v}{\partial t} = D_v\nabla^2 v + uv^2 - (\alpha+\beta)v. \tag{48}$$

The parameter α is feeding rate for u. The parameter β gives a kill or drain rate for v. The uv^2 term is a reaction term, producing v at the expense of u. In some ways the Gray-Scott model, looks and behaves remarkably similar to the Brusselator model.

Nice initial conditions (giving patterns) for the Gray-Scott model are $u = 1$, $v = 0$ and some locations in the v array set to 1.

A comprehensive site describing and illustrating (with videos!) phenomenology of the Gray-Scott reaction diffusion equation pattern formation model is here `http://www.mrob.com/pub/comp/xmorphia/index.html` where their F, k parameters, short for *feed, kill*, equals our α, β parameters, respectively.

1.8 The FitzHugh-Nagumo model

The reaction diffusion part of the FitzHugh-Nagumo are based on an excitable neuron. With appropriate values of the constants, rescaling and shifting of the fields and neglecting the diffusion terms, a special case of the system is equivalent to the Van der Pol oscillator which is discussed below!

A version of the FitzHugh-Nagumo model has

$$\begin{aligned} f_u(u,v) &= u - u^3 - v + \alpha \\ f_v(u,v) &= \beta(u-v) \end{aligned} \tag{49}$$

and

$$\begin{aligned} \frac{\partial u}{\partial t} &= D_u\nabla^2 u + f_u(u,v) \\ \frac{\partial v}{\partial t} &= D_v\nabla^2 v + f_v(u,v) \end{aligned} \tag{50}$$

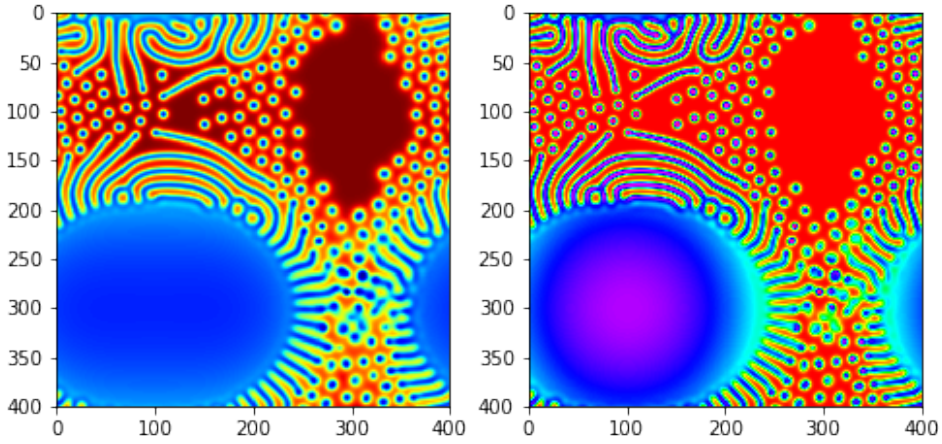

Figure 7: Patterns formed with the Gray-Scott model. u is on the left and v on the right. The grid has a sinusoidal variation in α (horizontally on the grid) and β (vertically on the grid). The mean values are $\alpha_m = 0.037$ and $\beta_m = 0.06$ with amplitudes of variation $\alpha_m/2$ and $\beta_m/8$. Diffusion coefficients are $D_u = 0.2, D_v = D_u/2$, the grid is $n = 400$ grid points and square and $\Delta x = \Delta t = 1$. Boundary conditions are periodic. The patterns grow but some regions of the plot (lower right) vary in time. In most regions, the patterns become fixed.

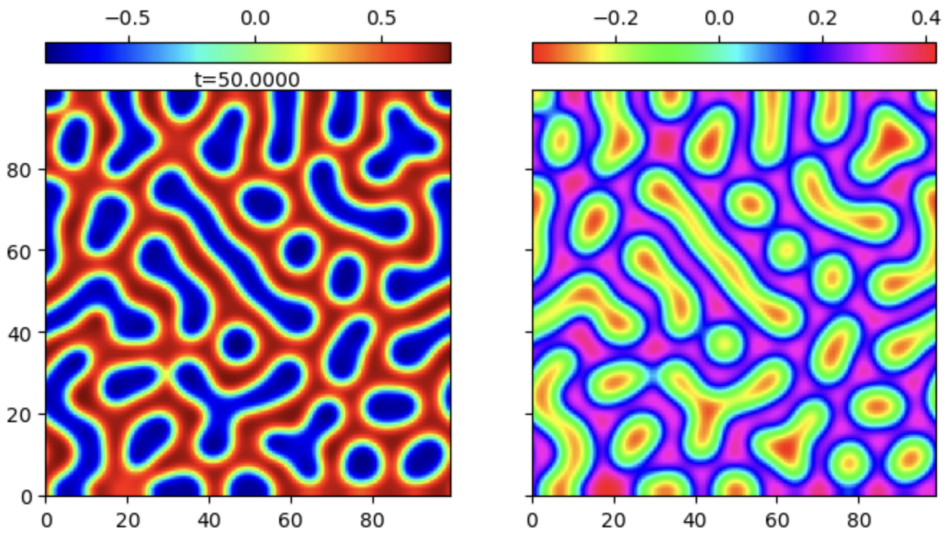

Figure 8: The FitzHugh-Nagumo model of equation 49 and 50 with $D_u = 1, D_v = 10, \alpha = 0.01, \beta = 1$ on a spatial grid with $dx = 1$ and updating with time-step $dt = 0.01$. The field u is on the left and v is on the right. The left and right boundaries are periodic, whereas the top and bottom are Neumann with normal component of gradient of the fields equal to zero.

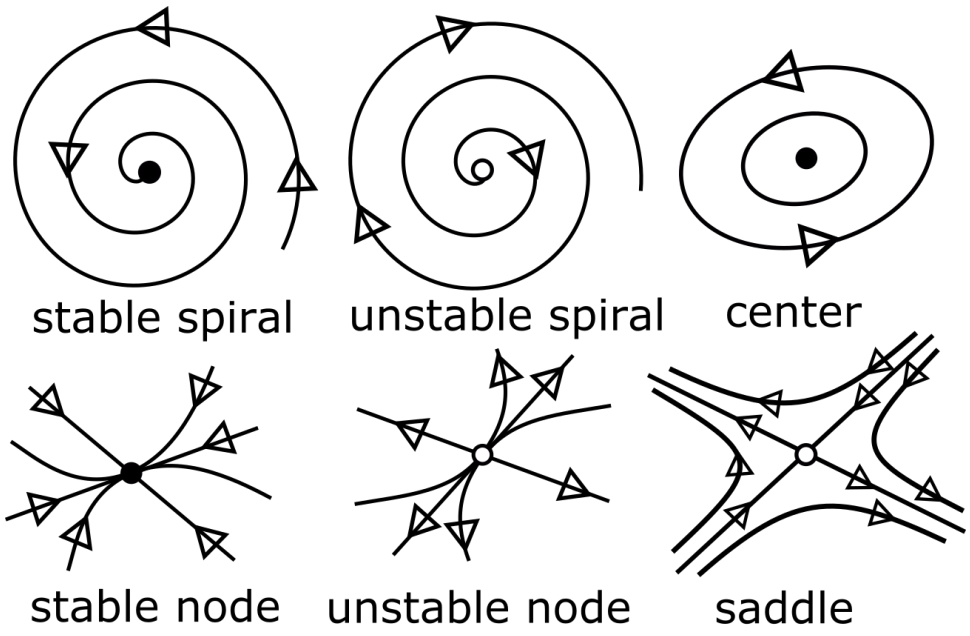

Figure 9: Different types of non-degenerate fixed points in 2-dimensional dynamical systems that are in the form $\dot{\mathbf{x}} = \mathbf{f}(\mathbf{x})$. The eigenvalues of the Jacobian matrix evaluated at the fixed point has imaginary components for the three systems in the top row. In the bottom row, both eigenvalues are different and real. Nodes are stable if the real part of both the eigenvalues are positive and unstable if they are both negative. If one eigenvalue is real and negative and the other is positive, the fixed point is a saddle node.

1.9 The Barkley model

The Barkley model is related to the Fitzhugh-Nagumo model. `http://www.scholarpedia.org/article/Barkley_model` The Barkley model depends on parameters a, b, ϵ and shows very pretty spirals!

$$\begin{aligned}
\partial_t u &= \delta u + f(u,v) \\
\partial_t v &= g(u,v) \\
f(u,v) &= \frac{1}{\epsilon} u(1-u)\left(u - \frac{v+b}{a}\right) \\
g(u,v) &= u - v.
\end{aligned} \tag{51}$$

2 Stability of fixed points in a 2-dimensional dynamical system

A dynamical system on the (x, y) can be described with a trajectory $(x(t), y(t))$. Consider the system

$$\begin{aligned}
\frac{dx}{dt} &= f(x,y) \\
\frac{dt}{dt} &= g(x,y)
\end{aligned}$$

specified by two functions $f(x, y)$ and $g(x, y)$.

A fixed point (x_*, y_*) satisfies

$$\begin{aligned}
f(x_*, y_*) &= 0 \\
g(x_*, y_*) &= 0.
\end{aligned} \tag{52}$$

We can look at the vicinity of the fixed point. Let's change variables to

$$\begin{aligned}
x &= x_* + u \\
y &= y_* + v
\end{aligned}$$

Because x_*, y_* are constants, $\frac{dx}{dt} = \frac{du}{dt}$ and $\frac{dy}{dt} = \frac{dv}{dt}$ The equation of motion becomes

$$\begin{aligned}
\frac{du}{dt} &= f(x_* + u, y_* + v) \approx f(x_*, y_*) + u\left.\frac{\partial f(x,y)}{\partial x}\right|_{(x_*,y_*)} + v\left.\frac{\partial f(x,y)}{\partial y}\right|_{(x_*,y_*)} \\
\frac{dv}{dt} &= g(x_* + u, y_* + v) \approx g(x_*, y_*) + u\left.\frac{\partial g(x,y)}{\partial x}\right|_{(x_*,y_*)} + v\left.\frac{\partial g(x,y)}{\partial y}\right|_{(x_*,y_*)}
\end{aligned}$$

Because (x_*, y_*) is a fixed point (equation 52) the equations of motion become

$$\frac{du}{dt} = u\frac{\partial f(x,y)}{\partial x}\bigg|_{(x_*,y_*)} + v\frac{\partial f(x,y)}{\partial y}\bigg|_{(x_*,y_*)}$$
$$\frac{dv}{dt} = u\frac{\partial g(x,y)}{\partial x}\bigg|_{(x_*,y_*)} + v\frac{\partial g(x,y)}{\partial y}\bigg|_{(x_*,y_*)}$$

to first order in u, v. In vector notation

$$\mathbf{u} = \begin{pmatrix} u \\ v \end{pmatrix}.$$

The Jacobian matrix

$$\mathbf{J}(x,y) = \begin{pmatrix} \frac{\partial f(x,y)}{\partial x} & \frac{\partial f(x,y)}{\partial y} \\ \frac{\partial g(x,y)}{\partial x} & \frac{\partial g(x,y)}{\partial y} \end{pmatrix}.$$

In matrix form the equation of motion near the fixed point is the linear dynamical system

$$\frac{d\mathbf{u}}{dt} = \mathbf{J}_*\mathbf{u}$$

where the matrix $\mathbf{J}_* = \mathbf{J}(x_*, y_*)$ is evaluated at the fixed point.

This is a linear system and its behavior depends on the eigenvalues of the matrix $\mathbf{J}_*$. We assume a solution in the form $\mathbf{u} = e^{\lambda t}\mathbf{w}$ with $\mathbf{w}$ a constant vector. We insert this into the equation of motion to find

$$\lambda\mathbf{w} = \mathbf{J}_*\mathbf{w}. \tag{53}$$

This implies that λ is an eigenvalue of $\mathbf{J}_*$ and $\mathbf{w} = (u_w, v_w)$ is its accompanying eigenvector.

As the matrix is a 2x2 matrix, there are two eigenvalues λ_1, λ_2. If λ_1 is real and positive then trajectories exponentially diverge from the fixed point along the direction specified by its eigenvector. If both λ_1, λ_2 are real and positive then the fixed point is a *repeller* and is called an *unstable node*. If both λ_1, λ_2 are real and negative then the fixed point is an *attractor* and is called a *stable node*. If one of the eigenvalues is positive and the other is negative then the fixed point is a *saddle node* and nearby trajectories resemble hyperbolas.

Equation 53 can be rewritten using the identity matrix as

$$(\mathbf{J}_* - \lambda\mathbf{I})\,\mathbf{w} = \begin{pmatrix} \frac{\partial f}{\partial x} - \lambda & \frac{\partial f}{\partial y} \\ \frac{\partial g}{\partial x} & \frac{\partial g}{\partial y} - \lambda \end{pmatrix} \begin{pmatrix} u_w \\ v_w \end{pmatrix} = 0 \tag{54}$$

where the derivatives are evaluated at the fixed point. This has a solution if and only if the determinant of the matrix $\mathbf{J}_* - \lambda\mathbf{I}$ is zero;

$$\begin{vmatrix} \frac{\partial f}{\partial x} - \lambda & \frac{\partial f}{\partial y} \\ \frac{\partial g}{\partial x} & \frac{\partial g}{\partial y} - \lambda \end{vmatrix} = 0. \tag{55}$$

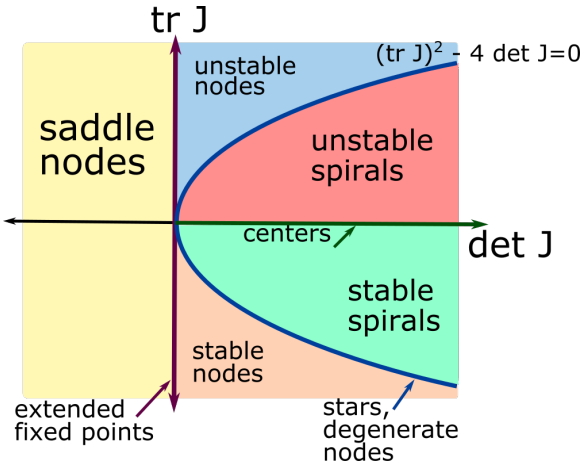

Figure 10: Classification of fixed points in 2-dimensional dynamical systems. J is the Jacobian matrix evaluated at the fixed point.

This gives the following equation which is called the *characteristic equation*

$$\lambda^2 - \left(\frac{\partial f}{\partial x} + \frac{\partial g}{\partial y}\right)\lambda + \frac{\partial f}{\partial x}\frac{\partial g}{\partial y} - \frac{\partial f}{\partial y}\frac{\partial g}{\partial x} = 0.$$

The characteristic equation can be written in terms of the trace of the Jacobian $\mathrm{tr}(\mathbf{J}_*)$ and the determinant of the Jacobian $\det(\mathbf{J}_*)$,

$$\lambda^2 - \mathrm{tr}(\mathbf{J}_*)\lambda + \det(\mathbf{J}_*) = 0.$$

The quadratic formula gives the eigenvalues

$$\lambda_1, \lambda_2 = \frac{1}{2}\mathrm{tr}(\mathbf{J}_*) \pm \frac{1}{2}\sqrt{(\mathrm{tr}(\mathbf{J}_*))^2 - 4\mathrm{det}\mathbf{J}_*}.$$

The general solution near the fixed point is

$$\mathbf{u} = \mathbf{c}_1 e^{\lambda_1 t}\mathbf{w}_1 + \mathbf{c}_2 e^{\lambda_2 t}\mathbf{w}_2$$

where $\mathbf{w}_1$ and $\mathbf{w}_2$ are the eigenvectors and constants $\mathbf{c}_1, \mathbf{c}_2$ are set by the initial condition. Note that there is a degenerate case; two eigenvectors might not exist.

If the eigenvalues have imaginary parts then these parts are equal and opposite in sign and there is rotation in the trajectories near the fixed point. If the real parts are positive and the eigenvectors have imaginary components then the fixed point is an unstable spiral or a spiral repeller. If the real parts are negative and the eigenvectors have imaginary components then the fixed point is a stable spiral node or a spiral attractor. If the eigenvalues are both imaginary (and the real parts are zero) then trajectories circle the fixed point and

the motion resembles that of a harmonic oscillator. See Figure 9 for some illustrations of non-degenerate cases.

There are some other annoying details: If both eigenvalues are zero, then a whole region is full of fixed points. If one eigenvalue is zero, there is a line of fixed points. There are degenerate nodes that are at the boundary between spiral and not spiral. These can have only a single eigenvector direction. If both eigenvalues are the same and are non-zero and there are two eigenvectors then the trajectories look like a star. The entire range of possibilities is shown in Figure 10.

3 Hopf bifurcation and the birth of limit cycles

A Hopf Bifurcation is a kind of bifurcation that only occurs in a two dimensional dynamical system. A limit cycle is born from a fixed point that becomes unstable.

A Hopf bifurcation is a system that is sensitive to a parameter that we can vary. As the parameter is varied, the stability of the fixed point changes its nature and a periodic solution is born. The fixed point loses its stability.

The eigenvalues of the Jacobian must be complex when the fixed point is unstable. The fixed point becomes a spiral repeller. If the map distant from the fixed point contracts, a stable and attracting periodic orbit known as a **limit cycle** is born.

3.0.1 The van der Pol oscillator

An example of a dynamical system that can exhibit a limit cycle is the van der Pol oscillator

$$\begin{aligned} \frac{dx}{dt} &= \mu(1-y^2)x - y \\ \frac{dy}{dt} &= x. \end{aligned} \tag{56}$$

The Jacobian matrix is

$$\mathbf{J}(x,y) = \begin{pmatrix} \mu(1-y^2) & -2\mu xy - 1 \\ 1 & 0 \end{pmatrix}. \tag{57}$$

The fixed point is at $(x,y) = (0,0)$. At the fixed point

$$\mathbf{J}(0,0) = \begin{pmatrix} \mu & -1 \\ 1 & 0 \end{pmatrix}. \tag{58}$$

Taking the determinant of $\mathbf{J}(0,0)$ we find the characteristic polynomial

$$\lambda^2 - \mu\lambda + 1 = 0,$$

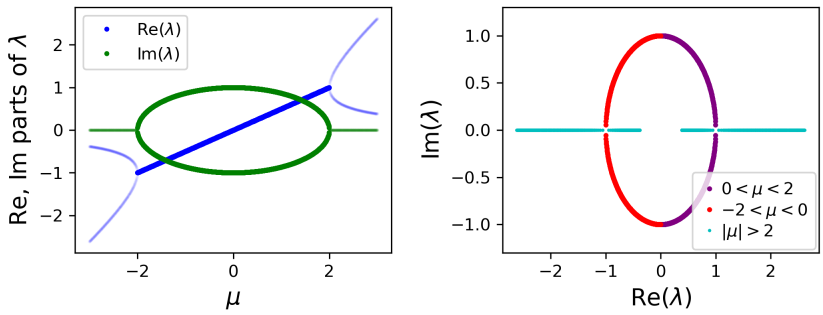

Figure 11: Eigenvalues of the Jacobian of the fixed point (computed using equation 59) of the van der Pol oscillator (with equation of motion in equation 56). Both eigenvalues are plotted on both plots. On the left we plot the real and complex part of the eigenvalues as a function μ. On the right we show the positions of the eigenvalues on the complex plane. The Hopf bifurcation occurs at $\mu = 0$ because just above this value of μ, the real component of the eigenvalues is positive. For $0 < \mu < 2$ the fixed point is an unstable spiral, and the system exhibits a limit cycle.

which has solutions

$$\lambda_1, \lambda_2 = \frac{\mu}{2} \pm \frac{1}{2}\sqrt{\mu^2 - 4}. \tag{59}$$

See Figure 11 for the behavior of real and complex parts of the eigenvalues.

As long as $|\mu| < 2$ there is an imaginary part. If $0 < \mu < 2$ the real parts of the eigenvalues are positive, there are imaginary parts and the fixed point is an unstable spiral node. If $-2 < \mu < 0$ the real part of the eigenvalues are negative, there are imaginary parts and the fixed point is a stable spiral node.

The fixed point makes a transition from a stable to an unstable one at $\mu = 0$. We say the Hopf bifurcation occurs at $\mu = 0$. We can consider the trajectories of the two eigenvalues on the complex plane as μ is increased. The eigenvalues cross the imaginary axis when $\mu = 0$ (see Figure 11 right plot). The limit cycle only exists for $0 < \mu < 2$.

Take a look at Figures 4 and 5 showing limit cycles in the Brusselator model.

4 The complex Ginzburg-Landau model

Many pattern forming models can be analyzed perturbatively by using equations called *amplitude equations*, which describe slow modulations in space and time of a simple basic pattern that can be determined from the linear analysis of the equations of motion of the physical system. This leads to a model that depends on a complex number, which is

equivalent to looking at evolution of an amplitude and a phase. In addition to the book by Cross and Greenside, there are review articles [4].

There are various forms of the complex Ginzburg-Landau equation for a field $A(\mathbf{x}, t) \in \mathbb{C}$ with $\mathbf{x} \in \mathbb{R}^d$. From Cross' book[5]

$$\partial_t A = A + (1 + ic_1)\nabla^2 A - (1 - ic_3)|A|^2 A. \tag{60}$$

From `https://codeinthehole.com/tutorial/index.html` (Winterbottom)

$$\partial_t A = A + (1 + i\alpha)\nabla^2 A - (1 + i\beta)|A|^2 A. \tag{61}$$

These two are the same PDE if you associate $\alpha = c_1$ and $\beta = -c_3$. From Chaté's and Manneville's 1996 review `https://arxiv.org/abs/1608.07519`

$$\partial_t A = A + (1 + ib_1)\nabla^2 A - (b_3 - i)|A|^2 A. \tag{62}$$

It is possible to convert between Chaté and Manneville's form and the other two.

Some transformations:

The complex Ginzburg Landau equation does not change if we make the transformation the transformation $A \to e^{i\alpha} A$ for some real phase α.

If we rescale the spatial coordinate $x \to \beta x$ then equation 62 becomes

$$\partial_t A = A + \beta^{-2}(1 + ib_1)\nabla^2 A - (b_3 - i)|A|^2 A. \tag{63}$$

If we rescale time $t \to \delta t$ then the equation becomes

$$\delta^{-1}\partial_t A = A + (1 + ib_1)\nabla^2 A - (b_3 - i)|A|^2 A. \tag{64}$$

If we rescale amplitude $A \to \gamma A$ then

$$\partial_t A = A + (1 + ib_1)\nabla^2 A - \gamma^2(b_3 - i)|A|^2 A. \tag{65}$$

A spatially dependent phase $A = e^{i\mathbf{k}\cdot\mathbf{x}}\psi$ gives

$$\begin{aligned} \nabla^2(e^{i\mathbf{k}\cdot\mathbf{x}}\psi) &= \nabla \cdot \nabla(e^{i\mathbf{k}\cdot\mathbf{x}}\psi) \\ &= \nabla \cdot (i\mathbf{k}e^{i\mathbf{k}\cdot\mathbf{x}}\psi + e^{i\mathbf{k}\cdot\mathbf{x}}\nabla\psi) \\ &= e^{i\mathbf{k}\cdot\mathbf{x}}\left(-k^2\psi + 2i\mathbf{k}\cdot\nabla\psi + \nabla^2\psi\right). \end{aligned} \tag{66}$$

[4] e.g., Pattern formation outside of equilibrium, M. Cross and P. Hohenberg, Reviews of Modern Physics, 65, 3, 1993, Chaté's and Manneville's 1996 review `https://arxiv.org/abs/1608.07519`. The world of the complex Ginzburg-Landau equation, Aranson and Kramer ,Reviews of Modern Physics, 74, 2002

[5] Pattern Formation and Dynamics in Non-equilibrium Systems, Michael Cross & Henry Greenside, Cambridge University Press, 2009.

We gain an advective term. We can go into a frame with a rotating phase by taking $A = e^{i\omega t}\psi$. Inserting this into equation 62 gives

$$\begin{aligned} i\omega\psi + \partial_t\psi &= \psi + (1+ib_1)\nabla^2\psi - (b_3 - i)|\psi|^2\psi \\ \partial_t\psi &= (1-i\omega)\psi + (1+ib_1)\nabla^2\psi - (b_3-i)|\psi|^2\psi. \end{aligned} \tag{67}$$

Equation 65 (rescaling amplitude) can be used to relate equation 61 to equation 62. We choose $\gamma = b_3^{-1/2}$ giving

$$\partial_t A = A + (1+ib_1)\nabla^2 A - (1 - ib_3^{-1})|A|^2 A. \tag{68}$$

Consequently if we choose

$$\alpha = b_1 \qquad \beta = -1/b_3 \tag{69}$$

we should have the same PDE models.

The real Ginzburg-Landau equation is with $c_1, c_3 = 0$ of equation 60 or $\alpha = \beta = 0$ of equation 61 giving $A \in \mathbb{R}$ and

$$\partial_t A = A + \nabla^2 A - A^3. \tag{70}$$

This has no free parameters! A coefficient on the Laplacian term can be removed via rescaling the spatial dimension. A coefficient on the time dependent term can be removed via rescaling time. A coefficient on one of the A or A^3 term can be removed via rescaling A.

When $b_1 \to \infty$, $b_3 = 0$ (using equation 62) dispersion is important and one recovers the non-linear Shrödinger equation.

In the above forms, the domain typically has size a few hundred so that interesting phenomena is seen.

5 The Swift-Hohenberg model

Reaction diffusion equations describe patterns developing with two fields. Pattern formation models exist for a single field, however with higher order derivatives. The Swift-Hohenberg model for $u(\mathbf{x}, t)$

$$\partial_t u = ru - (1+\Delta)^2 u - u^3. \tag{71}$$

This is derived for systems that are isotropic (the equation is invariant under $x \to -x$ and rotations) so lacks terms that depend upon ∇u.

We first discuss linear stability in the 1 dimensional case. In 1 dimension the operator of equation 71

$$(1+\Delta)^2 = 1 + 2\partial_{xx} + \partial_{xxxx}.$$

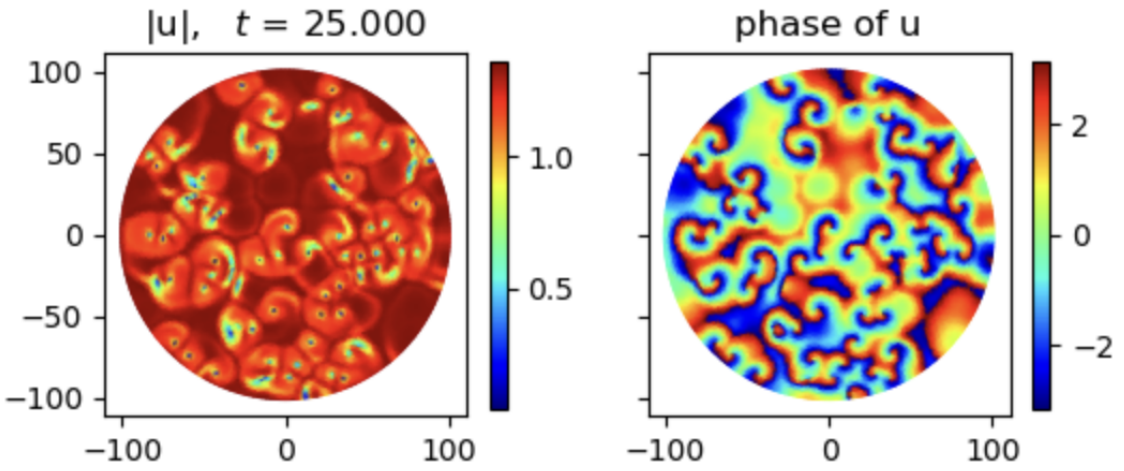

Figure 12: The complex Ginzburg-Landau model integrated on a triangular mesh with a Neumann boundary condition ($\nabla u \cdot \hat{\mathbf{n}} = 0$ on the boundary). The panel on the left shows the amplitude of the field and that on the right shows its phase. The model has $b_1 = 0, b_3 = 0.56$ and the timestep was $dt = 0.01$. The scheme was Crank-Nicolson for the Laplacian operator which was constructed with a finite element method. The non-linear term was added in afterwards with a forward Eulerian step.

The Swift-Hohenberg equation has a steady state solution $u(x,t) = 0$. We consider u small and insert a trial solution

$$u \propto e^{\sigma t + ikx}$$

which is wavelike in x. The wavevector k is related to wavelength via $k = 2\pi/\lambda$. Taking only first order terms after inserting our trial solution into the Swift-Hohenberg equation, we find

$$\sigma = r - (1 - k^2)^2. \tag{72}$$

If $\sigma > 0$ the solution will exponentially grow. We can consider the above equation as a function $\sigma(k)$ which has a maximum value at $k = 1$ which is equal to r. If $r > 0$ there are unstable solutions, with peak instability giving peak growth rates at a wavelength with $k = 1$ and growth rate equal to r.

A variant of the Swift-Hohenberg model includes a quadratic term with size controlled by an additional parameter γ_u

$$\partial_t u = ru - (1 + \Delta)^2 u + \gamma_u u^2 - u^3. \tag{73}$$

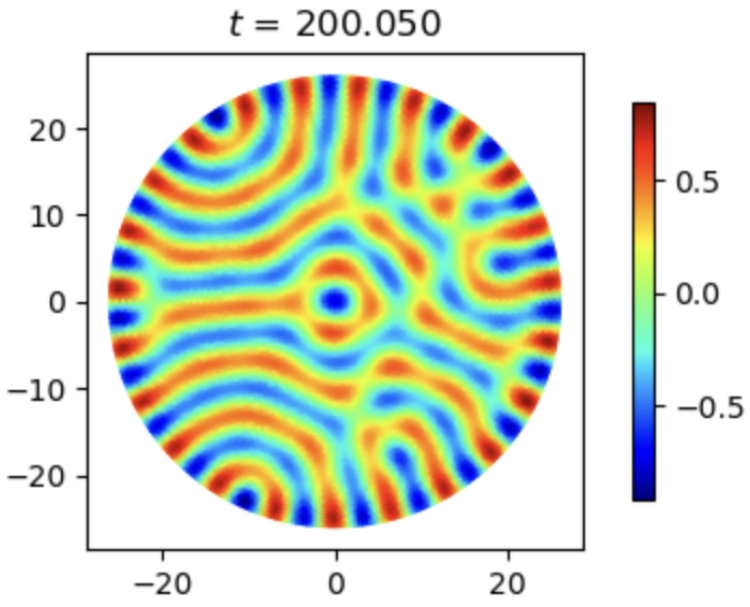

Figure 13: The Swift-Hohenberg model (equation 73) integrated on a triangular mesh in a circle with a natural boundary boundary (Neumann with normal gradient set to zero) and $r = 0.2, \gamma_u = 0$.

6 Practical issues and problems

The patterns that develop are dependent upon the initial conditions. For some models, like the Brusselator model, starting with initial conditions that look like noise (for example, drawn from a uniform or Gaussian distribution) is likely to give nice patterns. For other models, like the Gray-Scott model, you are better off setting a couple pixels to high values.

If your domain is too small or your pixel scale too big you may miss the patterns. You need to match your diffusion coefficients, pixel scale, and domain size so that the wavelength of the maximum growth rate fits nicely (is greater than the pixel scale but a few wavelengths smaller than your domain size). As is true for most diffusive numerical problems (using low order integration schemes), it is a good idea choose your timestep so that the time step is smaller than the rate that diffusion travels across a pixel.

I find that Dirichlet boundary conditions tend to kill the pattern growth (with the exception of the Gray Scott model), but Neumann boundary conditions (with gradient along the normal direction $\partial_n u = \partial_n v = 0$) makes fine patterns.

If you have a numerical way to compute the Laplacian operator (either using a Laplace-Beltrami operator) or via a finite element method, the models are fairly forgiving and you

be able to grow fine patterns on a mesh rather than on a Cartesian grid.

It is much hard to numerically implement the Swift-Hohenberg model because of the 4-th order biharmonic operator. On a periodic boundary and on a Cartesian square, I had success with a spectral method (transfer to Fourier space and do the Crank-Nicolson step in Fourier space instead of real space). On a triangular mesh I finally (with some effort). had success using a finite element method based on a Morley element and with a natural boundary condition.

6.1 Problems

In a triangular mesh, with Neumann boundary conditions, how does boundary size and shape affect the different models? (We have something to say about this now!)

How are models generalized on curved surfaces? (There is existing literature on this topic).

What happens if we slowly move the boundary mesh points?

How can we code more interesting boundary conditions? We can now have answered for the ones that only involved second order derivatives.